13th World Conference on Earthquake Engineering
Vancouver, B.C., Canada
August 1-6, 2004
Paper No. 2841

NUMERICAL ANALYSIS OF STRUCTURAL WALLS UNDER CYCLIC LOADS

Luca Sgambi[1], Luciano Catallo[2], Mehrdad Sasani[3]

SUMMARY

This paper studies analytical modeling of reinforced concrete (RC) structures subjected to cyclic loading. Special attention must be given to nonlinear material behavior when RC structures are subjected to cyclic loading. The material nonlinearity is due to characteristics such as: concrete orthotropic behavior, non symmetric material resistance (compression–tension), opening and closing cracks, and tension stiffening. In order to reliably predict the response of RC structures, the elements and the constitutive laws used in the analytical models must be able to properly account for these characteristics.

In this paper, a three-dimensional generalization of a membrane constitutive law [1] is used to model concrete cyclic behavior. The constitutive law is a rotating crack model, which considers concrete orthotropic behavior in each phase of loading (loading, unloading and reloading). The model is able to estimate, with good accuracy, the response of concrete under generic cyclic loads, accounting for opening and closing cracks. The material law has been implemented in a finite element program with an explicit formulation. Using the program, cyclic response of a structural wall is calculated and compared with the corresponding experimental results and a good agreement is achieved.

INTRODUCTION

In numerical analysis of RC structures under high cyclic stresses, it is important to account for orthotropic characteristics of concrete. There are concrete material models in the literature that consider orthotropic constitutive laws during the loading phase, but isotropic constitutive laws during the unloading or reloading phases [2]. Making use of the hypotheses available in the literature, notably established by Vecchio [1], and accounting for the orthotropic characteristics of concrete during the loading, unloading and reloading phases, a three-dimensional constitutive law has been formulated and implemented in a finite element program. This constitutive law is suitable for analyzing three-dimensional RC structures subjected to generic load histories. The formulation is based essentially on the compression field and the modified compression field theories [3], [4] and as a result the global response is calculated with reference to the response in the principal strain directions.

[1] Ph.D. Student, University of Rome “La Sapienza”, Rome, Italy. Email: luca.sgambi@uniroma1.it
[2] Ph.D. Student, University of Rome “La Sapienza”, Rome, Italy. Email: luciano.catallo@uniroma1.it
[3] Assistant Professor, Northeastern University, Boston, USA. Email: sasani@neu.edu

FINITE ELEMENT PROGRAM

The finite element program used in this paper was implemented in Fortran. This program is formulated in the displacement field, using 8-node isoparametric solid elements for concrete. In this paper the pseudo-static response of a RC structural wall is examined, however, first the general formulation for dynamic problems and the associated solution technique is described. Next the application of such formulation for static problems is discussed.

An explicit integration technique (central difference method) is used to solve the differential equation of motion of a nonlinear structure given by

$$\underline{\underline{M}} \cdot \underline{\ddot{U}} + \underline{\underline{C}} \cdot \underline{\dot{U}} + \underline{F} = \underline{R} \qquad (1)$$

where $\underline{\underline{M}}$ and $\underline{\underline{C}}$ are the mass and damping matrices of the structure, respectively. $\underline{U}$, $\underline{F}$, and $\underline{R}$ are the relative displacement, internal and external nodal force vectors, respectively. Note that in a linear structure $\underline{F}$ can be replaced by $\underline{\underline{K}}\ \underline{U}$, where $\underline{\underline{K}}$ is the stiffness matrix of the structure.

Using the central difference method, (1) can be written as

$$\left(\frac{1}{\Delta t^2}\underline{\underline{M}} + \frac{1}{2\Delta t}\underline{\underline{C}}\right) \cdot \underline{U}^{i+1} = \underline{R}^i - \underline{F}^i - \frac{2}{\Delta t^2}\underline{\underline{C}} \cdot \underline{U}^i - \left(\frac{1}{\Delta t^2}\underline{\underline{M}} - \frac{1}{2\Delta t}\underline{\underline{C}}\right) \cdot \underline{U}^{i-1} \qquad (2)$$

where the superscript i represents the discrete time instance t_i and $\Delta t = t_i - t_{i-1}$. In (2) both the mass and damping matrices are constant at all times, while the resisting internal forces ($\underline{F}^i$) need to be updated, given the nonlinear material behavior. If in a structural model the mass is idealized as lumped masses at the nodes of the discretized structure and the damping matrix is considered to be proportional to the mass matrix,

$$\underline{\underline{C}} = \alpha \underline{\underline{M}} \qquad (3)$$

the resulting matrix in the parentheses on the left hand side of (2) becomes diagonal and $\underline{U}^{i+1}$ can be calculated from a set of uncoupled linear equations. In other words, there will be no need for inverting large non diagonal matrices in this approach. Of course, one needs to keep in mind that the central difference method is only conditionally stable and requires a time step Δt smaller than a critical time step. Therefore, compared to implicit integration techniques such as the Newmark method, a larger number of steps may be required to find the solution using the central difference method.

The resisting internal forces for element n at the end of the step i is

$$F_n^i = \underline{\underline{B}}_n^T \cdot \underline{\underline{D}}_n^i \cdot \underline{\varepsilon}_n^i \qquad (4)$$

where the matrix $\underline{\underline{B}}_n$ contains the derivatives of the shape functions and $\underline{\underline{D}}_n^i$ relates stresses to strains ($\sigma_n^i = \underline{\underline{D}}_n^i \cdot \underline{\varepsilon}_n^i$). It should be noted that given the material nonlinearity, the matrix $\underline{\underline{D}}_n^i$ is not constant and has to be updated at each step.

The explicit integration technique described above can be used in solving static problems [5]. Such a technique is effective for solving nonlinear problems with a large numbers of degrees of freedom, and simplifies the numerical solution for structures under cyclic loading.

MATERIAL MODEL

Concrete material model

The material law for concrete consists of three parts:

- Envelope law
- Unload-reload law
- Residual strain law

It is assumed that the envelope curve follows monotonic stress-strain relationships. Under compressive strain, the equation proposed by Elwi [6] is used,

$$\sigma_j = R_{cj} \frac{K_j\left(\dfrac{\varepsilon_{uj}}{\varepsilon_{cj}}\right)}{1 + A_j\left(\dfrac{\varepsilon_{uj}}{\varepsilon_{cj}}\right) + B_i\left(\dfrac{\varepsilon_{uj}}{\varepsilon_{cj}}\right)^2 + C_i\left(\dfrac{\varepsilon_{uj}}{\varepsilon_{cj}}\right)^3} \qquad \text{(j=1, 2, 3)} \qquad (5)$$

where the subscript *j* indicates the principal direction. The definitions of the terms can be found in [6] and [7]. Under tensile strain, the following envelope law is used:

$$\sigma_j = \begin{cases} E_0 \cdot \varepsilon_j & if \quad \varepsilon_j < \varepsilon_{cr} \\ \dfrac{E_0 \cdot \varepsilon_{cr}}{1+\sqrt{500 \cdot \varepsilon_j}} & if \quad \varepsilon_j > \varepsilon_{cr} \end{cases} \qquad (6)$$

which is based on experimental results and accounts for the tension stiffening effect due to the presence of the reinforcement bar in the concrete. In (6), ε_{cr} is the concrete cracking strain and E_0 is the initial elastic modulus [4]. Note that tensile strain is positive.

The expression used to describe the unload-reload phase in compression, is [1]:

$$\sigma_j = \begin{cases} 0 & if \quad \varepsilon_{cj} > \varepsilon_{cj}^r \\ (\varepsilon_{cj} - \varepsilon_{cj}^r) \cdot \dfrac{\sigma_{cjm}}{\varepsilon_{cim} - \varepsilon_{cj}^r} & if \quad \varepsilon_{cj}^r > \varepsilon_{cj} > \varepsilon_{cjm} \end{cases} \qquad (7)$$

where ε_{cj}^r is the residual compressive strain and ε_{cjm} is the largest compressive strain calculated along the direction examined. Note that the unload-reload law in compression is simply made of two lines that join the point (*0,0*) with the point (*0*, ε_{cj}^r) and the point (*0*, ε_{cj}^r) with the point (σ_{cjm}, ε_{cjm}). The unload-reload in tension is described by the following secant law:

$$\sigma_j = \frac{\varepsilon_{tj} \cdot \sigma_{tjm}}{\varepsilon_{tjm}} \qquad (8)$$

which represents a line that connects the point ($\sigma_{tjm}, \varepsilon_{tjm}$) to the origin (*0,0*). The subscript *m* in (8) represents the largest value of the corresponding strain reached during the previous load history. The corresponding stress component (that has again the index *m*) is calculated by the envelope law. In Figure 1, a schematic representation of these hypotheses is shown.

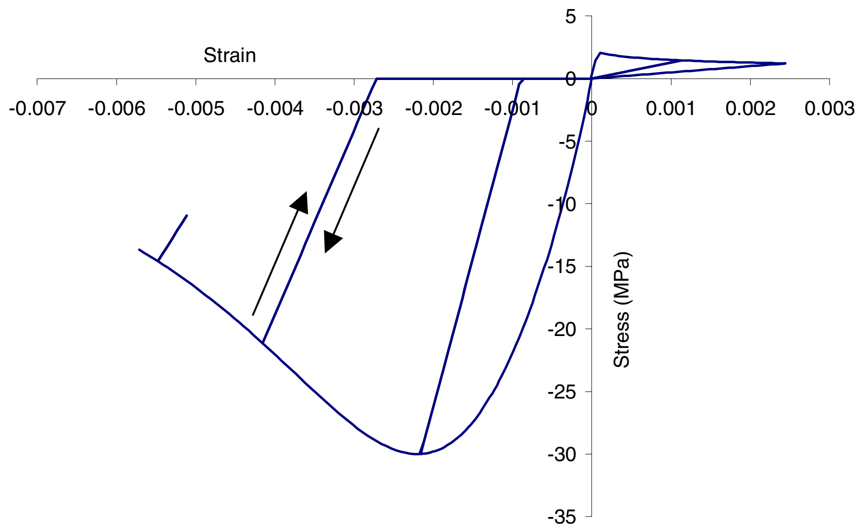

Figure 1: Loading and reloading curves

The implemented model considers a residual strain in the compression state only. The value of the residual strain is

$$\varepsilon_{cj}^{r} = \varepsilon_{cj} - \frac{\sigma_{cj}}{\omega \cdot E_0} \tag{9}$$

where the point ($\varepsilon_{cj}, \sigma_{cj}$) is on the envelope curve and E_0 is the initial elastic modulus. The ω coefficient adjusts the slope of the unload-reload branch.

In two and three dimensional problems, the definitions of unload and reload are made utilizing an updated tensor of the maximum tensile strains and a tensor of residual compressive strains at each step. These tensors are given in the Cartesian coordinates, but the updating is carried out in the current principal coordinates. Therefore, for each load step, the principal directions of strains are calculated and both tensors are transformed (rotated) to the current principal coordinates. Then, if it is necessary, the diagonal terms are updated as shown in (10). Note that in (10) the subscript *m* refers to the maximum strain tensors while the subscript *i* refers to the strain tensors in step *i*. In this process, only the diagonal terms are updated and the non diagonal terms are considered zero. This is a hypothesis that simplifies the updating process. After updating, the tensors are transformed into the Cartesian coordinates.

$$\left.\begin{array}{l}\begin{bmatrix}\varepsilon_{xx} & \varepsilon_{xy} & \varepsilon_{xz}\\ \varepsilon_{yx} & \varepsilon_{yy} & \varepsilon_{yz}\\ \varepsilon_{zx} & \varepsilon_{zy} & \varepsilon_{zz}\end{bmatrix}_i \equiv \begin{bmatrix}\varepsilon_{11} & 0 & 0\\ 0 & \varepsilon_{22} & 0\\ 0 & 0 & \varepsilon_{33}\end{bmatrix}_i \\ \\ \begin{bmatrix}\varepsilon_{xx} & \varepsilon_{xy} & \varepsilon_{xz}\\ \varepsilon_{yx} & \varepsilon_{yy} & \varepsilon_{yz}\\ \varepsilon_{zx} & \varepsilon_{zy} & \varepsilon_{zz}\end{bmatrix}_m \equiv \begin{bmatrix}\tilde{\varepsilon}_{11} & \tilde{\varepsilon}_{12} & \tilde{\varepsilon}_{13}\\ \tilde{\varepsilon}_{21} & \tilde{\varepsilon}_{22} & \tilde{\varepsilon}_{23}\\ \tilde{\varepsilon}_{31} & \tilde{\varepsilon}_{32} & \tilde{\varepsilon}_{33}\end{bmatrix}_m\end{array}\right\} \begin{bmatrix}\varepsilon_{11} \;\; if \;\; \varepsilon_{11} > \tilde{\varepsilon}_{11} & 0 & 0\\ 0 & \varepsilon_{22} \;\; if \;\; \varepsilon_{22} > \tilde{\varepsilon}_{22} & 0\\ 0 & 0 & \varepsilon_{33} \;\; if \;\; \varepsilon_{33} > \tilde{\varepsilon}_{33}\end{bmatrix}_m \tag{10}$$

In order to transform strains between the principal and Cartesian coordinates two rotation matrices are needed. $\underline{\underline{T}}_1$ is used for rotating the tensors from the principal axes to the Cartesian axes and $\underline{\underline{T}}_2$ is used for rotating from the Cartesian axis to the principal axis. If the tensors are presented in vectorial forms, these rotation matrices have the following form

$$\underline{\underline{T}}_1 = \begin{bmatrix} l_1^2 & m_1^2 & n_1^2 & l_1 \cdot m_1 & m_1 \cdot n_1 & l_1 \cdot n_1 \\ l_2^2 & m_2^2 & n_2^2 & l_2 \cdot m_2 & m_2 \cdot n_2 & l_2 \cdot n_2 \\ l_3^2 & m_3^2 & n_3^2 & l_3 \cdot m_3 & m_3 \cdot n_3 & l_3 \cdot n_3 \\ 2 \cdot l_1 \cdot l_2 & 2 \cdot m_1 \cdot m_2 & 2 \cdot n_1 \cdot n_2 & l_1 \cdot m_2 + l_2 \cdot m_1 & m_1 \cdot n_2 + m_2 \cdot n_1 & n_1 \cdot l_2 + n_2 \cdot l_1 \\ 2 \cdot l_2 \cdot l_3 & 2 \cdot m_2 \cdot m_3 & 2 \cdot n_2 \cdot n_3 & l_2 \cdot m_3 + l_3 \cdot m_2 & m_2 \cdot n_3 + m_3 \cdot n_2 & n_2 \cdot l_3 + n_3 \cdot l_2 \\ 2 \cdot l_3 \cdot l_1 & 2 \cdot m_3 \cdot m_1 & 2 \cdot n_3 \cdot n_1 & l_3 \cdot m_1 + l_1 \cdot m_3 & m_3 \cdot n_1 + m_1 \cdot n_3 & n_3 \cdot l_1 + n_1 \cdot l_3 \end{bmatrix} \tag{11}$$

The coefficients l_i, m_i, and n_i, are the direction cosines of the principal coordinates and can be evaluated from the strain tensor in each step using a Jacoby procedure. The matrix $\underline{\underline{T}}_2$ is found using the direction cosines of the Cartesian axes with respect to the principal coordinate system.

Defining the following vectors in the Cartesian coordinates:

$\underline{\varepsilon}_{tm}^{xyz}$: maximum tensile strain vector

$\underline{\varepsilon}_{cm}^{xyz}$: maximum compressive strain vector

$\underline{\varepsilon}_{cr}^{xyz}$: maximum residual compressive strain vector

stresses in concrete are evaluated taking the following steps:

- Evaluate current principal strain and the corresponding coordinate system using a Jacobi procedure.
- Transform the maximum and residual strains into the current principal system:

$$\underline{\varepsilon}_{tm}^{123} = \underline{\underline{T}}_2 \cdot \underline{\varepsilon}_{tm}^{xyz}; \qquad \underline{\varepsilon}_{cm}^{123} = \underline{\underline{T}}_2 \cdot \underline{\varepsilon}_{cm}^{xyz}; \qquad \underline{\varepsilon}_{cr}^{123} = \underline{\underline{T}}_2 \cdot \underline{\varepsilon}_{cr}^{xyz} \tag{12}$$

- Evaluate concrete stresses using the uniaxial laws defined by Equations (5) to (8).
- Update the maximum and residual strains in the current principal coordinates in accordance with (10)
- Transform (rotate) the concrete stresses as well as the maximum and residual strains into the Cartesian coordinates

$$\underline{\varepsilon}_{tm}^{xyz} = \underline{\underline{T}}_1 \cdot \underline{\varepsilon}_{tm}^{123}; \qquad \underline{\varepsilon}_{cm}^{xyz} = \underline{\underline{T}}_1 \cdot \underline{\varepsilon}_{cm}^{123}; \qquad \underline{\varepsilon}_{cm}^{xyz} = \underline{\underline{T}}_1 \cdot \underline{\varepsilon}_{cm}^{123}; \qquad \underline{\sigma}^{xyz} = \underline{\underline{T}}_1 \cdot \underline{\sigma}^{123} \tag{13}$$

Figure 2 depicts the main procedures implemented in the finite element program. In Figure 3(a) the failure surface for biaxial normal stresses (Kupfer experimental results) and in Figure 3(b) the failure ranges for normal-shear stresses (Bresler-Pister experimental results) are shown. The experimental results are shown in dotted lines while the predictions based on the analytical models implemented here are shown in solid lines. As it can be seen there are reasonable agreements between the experimental and the analytical results.

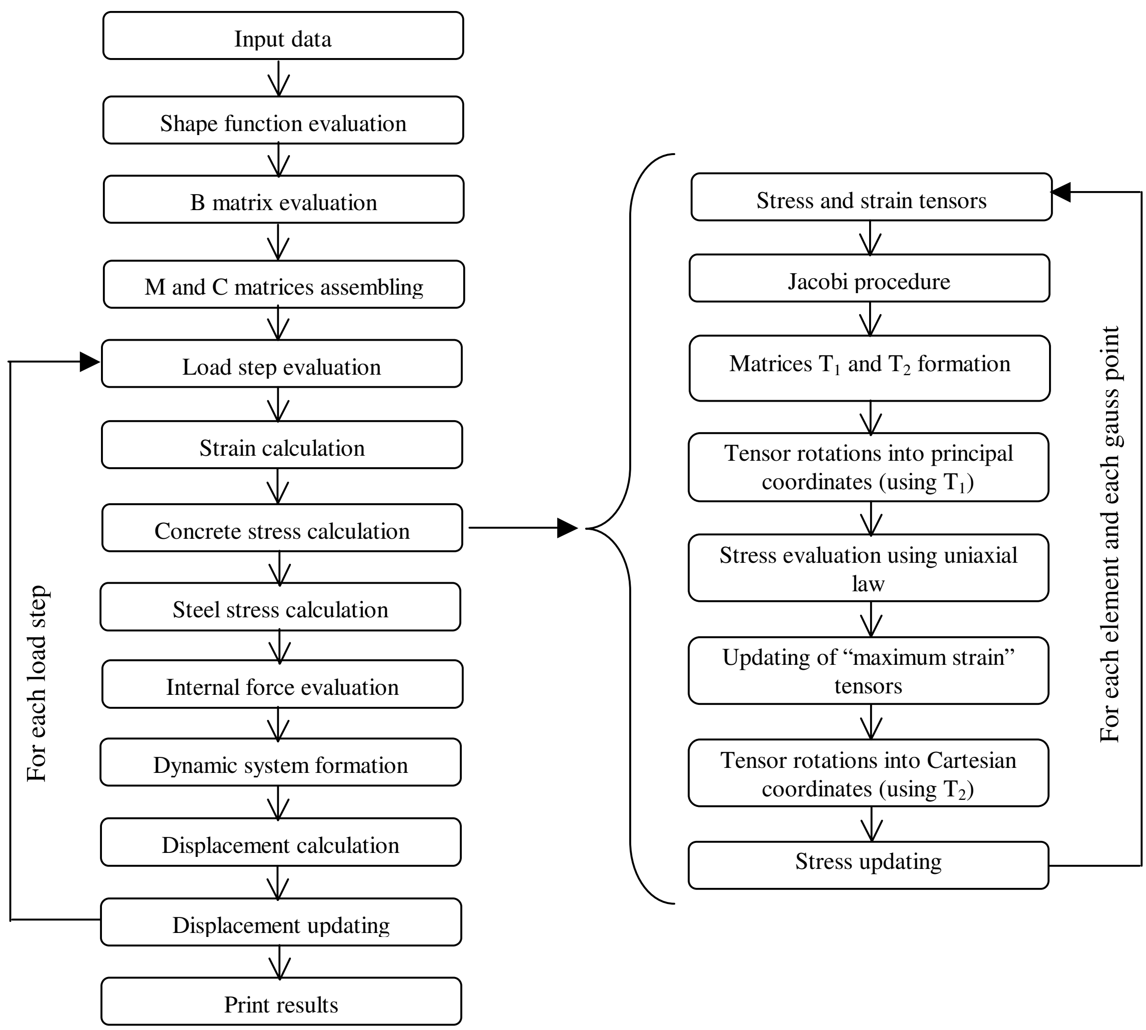

Figure 2. Flow-chart of finite element program and flow-chart of concrete material law

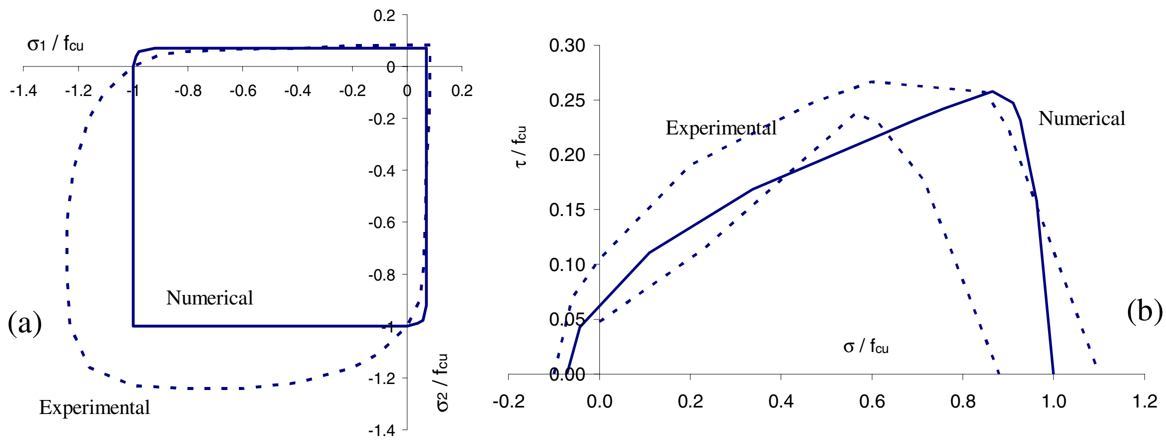

Figure 3. Experimental and numerical failure curves

Steel material model
The nonlinear stress-strain relationship of the steel bars is assumed bilinear with kinematic hardening. Figure 4 shows the form of the cyclic stress-strain relationship for steel bars.

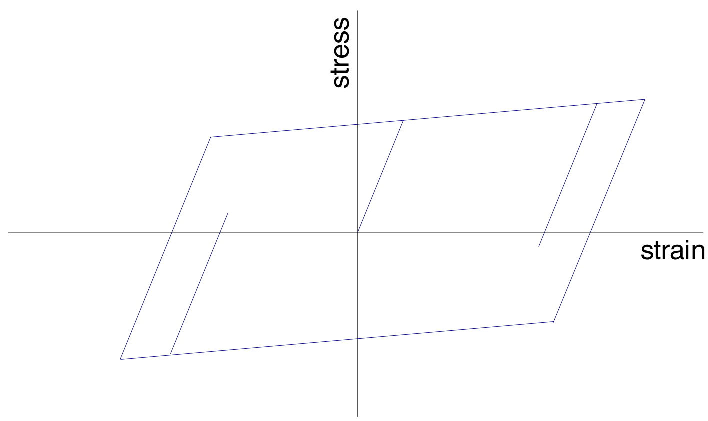

Figure 4: Cyclic stress-stain relationship for steel bars

In order to account for the concentration of stress in steel bars at crack locations and variation of stress between cracks as a result of surrounding concrete, a modified value for the steel yield stress, $f_y^{'}$, is used [8], [9]

$$f_y^{'} = \left(0.93 - 2 \cdot \frac{1}{\rho} \cdot \left(\frac{f_{cr}}{f_y}\right)^{1.5}\right) \cdot f_y \qquad (14)$$

where f_{cr} is the tensile cracking stress of concrete and ρ is the longitudinal reinforcement ratio.

The reinforcing bars are considered smeared into the concrete. In order to account for the steel bar stress in the model, the stress of a composite material is used

$$\underline{\sigma} = \underline{\sigma}_{concrete} + \underline{\tilde{\sigma}}_{steel} \tag{15}$$

where $\underline{\tilde{\sigma}}_{steel}$ is found by multiplying the steel stress and the steel reinforcement ratio of the element under consideration.

ANALYSIS OF A STRUCTURAL WALL

In order to validate the analytical procedure presented in this paper, the experimental test results of a structural wall is examined. The wall B2 tested by Oesterle [10] is *1910 mm* wide and *4570 mm* tall. The thickness of the web is *102 mm*. The dimensions of the square boundary elements is *305 mm.* A description of the wall geometry and its finite element model are given in Figure 5.

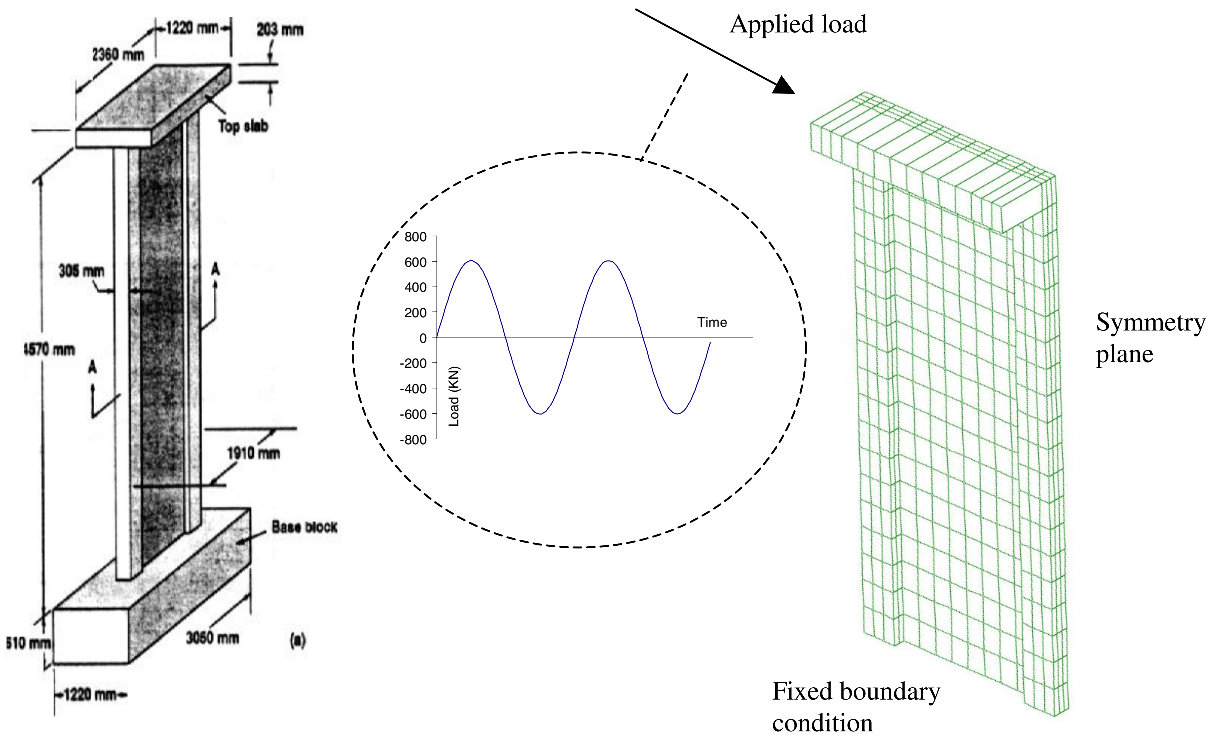

Figure 5: Geometry [1] and finite element model of Wall B2

The characteristics of the reinforcement are reported in Table 1. The concrete compressive strength is reported equal to *53.7 MPa*. The wall is subjected to cyclic shear forces at the top. Note that the cyclic load causes a continuous rotation of stress and strain tensors and, for this reason, this test results allows to examine the validity of the hypothesis described in the analytical modeling.

Table 1: Steel reinforcement characteristics

Zone	Horizontal reinforcement		Vertical reinforcement	
	Percentage	f_y (MPa)	Percentage	f_y (MPa)
Web	0.63	533	0.29	533
Boundary Elements	0.63	533	3.67	410

In the numerical analysis, one full cycle of the load is applied in *30* sec and in order to have stability and accuracy, $\Delta t=0.0001$ sec is used. In Figure 6, the numerical solution is compared with the experimental results. As it can be seen, a good agreement is achieved. Note that because the effect of confining reinforcement in the boundary elements was not accounted for, the analysis was continued until there was a need for distinguishing between the behavior of the core and the cover concrete.

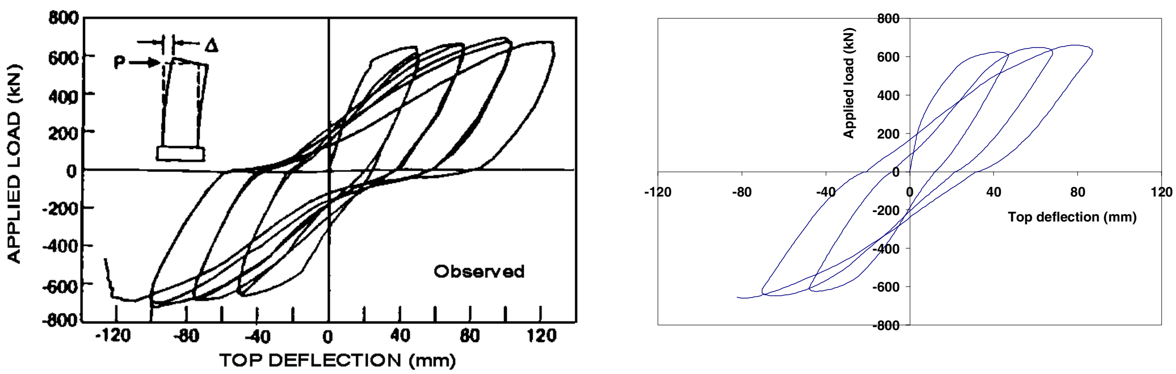

Figure 6: Experimental [10] and numerical response for wall B2

CONCLUSIONS

A numerical algorithm is presented for analyzing three dimensional RC structures under general loading conditions. The concrete material model is based on a three dimensional generalization of membrane theories [4], [1]. The material model used to update the concrete properties under cyclic loads considers both the response along the principal directions and the change of the principal coordinate system during the cyclic loading. The response of a reinforced concrete wall was investigated in order to validate the algorithm. The analytical results are in good agreements with the experimental results.

AKNOWLEDGEMENTS

The financial support of COFIN2002 and University of Rome "La Sapienza" is acknowledged. The support of Professor Franco Bontempi (University of Rome "La Sapienza") and Professor Ali Touran (Northeastern University of Boston) is also appreciated.

REFERENCES

1. Vecchio FJ. "Towards cyclic load modeling of reinforced concrete," ACI Structural Journal, 1999; 96(2): 193-202.

2. Balan TA, Filippou FC, Popov EP. “Constitutive model for 3D cyclic analysis of concrete structures.” Journal of Engineering Mechanics 1997; 123(2): 143-153.
3. Vecchio FJ, Collins MP. “Compression response of cracked reinforced concrete.” Journal of the Engineering Mechanics Division, ASCE, 1973; 119(12): 3590-3610.
4. Vecchio FJ. “Nonlinear finite element analysis of reinforced concrete membranes.” ACI Structural Journal, 1989; 86(1): 26-35.
5. Zienkiewicz OC. Taylor RL. The Finite Element Method, 4th Edition, Vol.2, *McGraw Hill*, 1989.
6. Elwi AA, Murray DW. “A 3D hypoelastic concrete constitutive relationship.” Journal of the Engineering Mechanics Division, ASCE, 1979; 105(4): 623-641.
7. Darwin D, Pecknold DA. “Nonlinear biaxial stress-strain law for concrete.” Journal of the Engineering Mechanics Division, ASCE, 1979; 103(2): 229-241.
8. Hsu TCC. Unified theory of reinforced concrete. *CRC Press*, 2000.
9. Hsu TTC. "Concrete stiffness matrices for membrane elements." Structural Engineering and Mechanics, Techno-Press, 1997; 5(5): 599-608.
10. Oesterle RG, Fiorato AE, Johal LS, Carpenter JE, Russell HE, Corley WG. Earthquake resistance structural walls—tests of isolated walls, Construction Technology Laboratories, PCA, Skokie, IL, 1976.